

## Ecofriendly CuO@CaO@Fe<sub>3</sub>O<sub>4</sub> nanocomposite using *Juglans regia L.* walnut green husk extract — synthesis and biological applications



Zagros

Abdulrahman Omar<sup>1</sup>

Rawen Hasan

Mahmud<sup>1</sup>

Sima Sherzad Omer<sup>1</sup>

Rihan Saadi Abdul

Jabar<sup>2,3</sup>

Abdelaal Sayed

Abdelaal Ahmed<sup>4</sup>

Gomaa Abdelgawad

Mohammed Ali<sup>4,5</sup>

<sup>1</sup>Chemistry Department, Soran University, Soran-Erbil, Kurdistan Region, Iraq.

<sup>1</sup>Email: [zagros.omar@soran.edu.iq](mailto:zagros.omar@soran.edu.iq)

<sup>1</sup>Email: [rh4020@chem.soran.edu.iq](mailto:rh4020@chem.soran.edu.iq)

<sup>1</sup>Email: [ss3520@chem.edu.iq](mailto:ss3520@chem.edu.iq)

<sup>2</sup>Cihan University – Duhok, College of Health Sciences, Department of Clinical Biochemistry, Duhok, Iraq.

<sup>2</sup>Email: [rihan.abduljabar@visitor.duhokcihan.edu.krd](mailto:rihan.abduljabar@visitor.duhokcihan.edu.krd)

<sup>3</sup>Department of Chemistry, College of Science, University of Zakho, Zakho, Kurdistan Region, Iraq.

<sup>4</sup>Chemistry Department, Faculty of Science, Al-Azhar University, Assiut 71524, Egypt.

<sup>4</sup>Email: [abdelaalsayed@gmail.com](mailto:abdelaalsayed@gmail.com)

<sup>5</sup>College of Marine Science and Aquatic Biology, University of Khorfakkan, Khorfakkan, 18119, Sharjah, United Arab Emirates.

<sup>5</sup>Email: [gomaasanad@gmail.com](mailto:gomaasanad@gmail.com)



(+ Corresponding author)

## ABSTRACT

### Article History

Received: 1 September 2025

Revised: 16 December 2025

Accepted: 21 January 2026

Published: 3 February 2026

### Keywords

Antibacterial activity

Antioxidant activity

CuO@CaO@Fe<sub>3</sub>O<sub>4</sub>

Green nanotechnology

Green synthesis

*Juglans Regia L.*

Nanocomposite

Phytochemicals

Polyphenolics quantification

Walnut green husk.

During the processing of *Juglans regia L.*, a large quantity of walnut green husk is produced as an agricultural byproduct. This residue exhibits significant biological importance, especially considering its natural antibacterial properties, which indicate its potential as a natural alternative to conventional antibiotics. In this work, the green husk of *J. regia* was extracted and characterized for its phytochemical profile, antioxidant potential, and content of total phenolics and flavonoids. It was then used as a reducing and stabilizing agent in the green synthesis of a CuO@CaO@Fe<sub>3</sub>O<sub>4</sub> nanocomposite, resulting in nanoparticles approximately 90 nm in size. Phytochemical screening revealed that the extract contains diverse classes of bioactive molecules, including diterpenes, steroids, triterpenoids, coumarins, flavonoids, and various polyphenolic compounds. Quantitatively, phenolic compounds (62.67 µg GAE/500 µg extract) and flavonoids (38.61 µg QE/500 µg extract) are the predominant chemical categories. These naturally occurring molecules effectively coat the surface of the nanocomposite, significantly enhancing its antioxidant activity, with hydrogen peroxide scavenging ability surpassing that of vitamin C. Additionally, the synthesized CuO@CaO@Fe<sub>3</sub>O<sub>4</sub> nanocomposite demonstrated notable antibacterial activity. In vitro assays confirmed its efficacy against both Gram-negative and Gram-positive bacterial strains, indicating promising prospects for biomedical and antimicrobial applications.

**Contribution/ Originality:** This study contributes to the literature by developing an eco-friendly CuO@CaO@Fe<sub>3</sub>O<sub>4</sub> nanocomposite using *Juglans regia L.* walnut green husk extract. This study employs green synthesis methodology and is among the few studies that have investigated its antioxidant and antibacterial applications. It documents the biological potential of the CuO@CaO@Fe<sub>3</sub>O<sub>4</sub> nanocomposite.

## 1. INTRODUCTION

Recently, nanocomposites, which include many phases, exhibit remarkable qualities, attracting significant scientific interest due to their distinctive design and novel characteristics [1]. Consequently, these have demonstrated their usefulness in a variety of fields, including bioengineering, sensing, catalysis, and renewable energy, since they can overcome the drawbacks of single-phase or micro-composites [2-5]. Usually, composite nanomaterials are synthesized through the integration of secondary phases with either the external or internal surfaces of components. These methods include sol-gel, hydrothermal, chemical vapor deposition, and solution mixing [2]. However, these methods still have some limitations, such as controlling the chemical composition, stoichiometry, and architecture. Historically, plants have been extensively used in textiles, cosmetics, biomedicine, food, and medicine. As a result of technological advancements and new platforms, the biomedical uses of plants have grown dramatically in recent decades [6, 7]. One of the most fascinating aspects of plants is their phytochemicals, which include antibacterial, anticancer, anti-aging, and other qualities, and are mainly responsible for these biological activities [8, 9]. Therefore, understanding or utilizing phytochemicals for more applications has received great attention in research. Many studies conducted in recent years have focused on preparing nano-based materials from phytochemicals in plant extracts, as this approach is less harmful to the environment than conventional methods [10, 11].

The Juglandaceae family includes walnut *Juglans regia L.* (*J. regia L.*), which is primarily grown in poor and unreclaimed soils. The main countries involved in walnut production are the United States, Iran, Turkey, and China [12]. Various components of walnuts, including the green husk, shells, bark, kernels, seeds, and leaves, have significant applications in cosmetics and medicine [13, 14].

The greenery is extensively used in medicine for its astringent, antiseptic, antidiarrheal, and anthelmintic properties, as well as for skin treatment [15]. To remove heavy metals from aqueous solutions, the outer layer is frequently utilized as charcoal [16] and as a catalyst in renewable energy systems.

Rarely recycled, walnuts are the primary byproduct of walnut production, making up over half of the entire fruit. The green husk of the walnut contains polyphenol chemicals. Typically, walnut contains thirteen distinct phenolic compounds, namely gallic acid, protocatechuic acid, ellagic acid, epicatechin, vinyl acid, catechin, juglone, and myricetin; these make up 30% of the green husk's phenolic compounds [17]. Walnut *J. regia L.* is usually used as an alternative medicine as an antibacterial, carminative, anthelmintic, astringent, tonic, and hypoglycemic agent [18]. The green leaves of *J. regia L.* are conventionally employed in medicinal practices for the treatment of rheumatic pain and fever. *J. regia L.* has also been used to treat diabetes, heart illness, inflammation, and lung cancers, as a source of bioactive phytochemicals [19].

The green synthesis of nanocomposite materials is crucial as it offers an eco-friendly, sustainable, and economical method for producing cutting-edge materials with minimal toxic byproducts, aligning with global efforts to reduce environmental impact and promote green chemistry [20, 21].

More recently, excellent research has been focused on greening various nanomaterials using walnut and its extracts. For instance, Erdem and Çakır [22] synthesized silver nanoparticles (Ag NPs) with an average particle size of 109 nm utilizing extracts from walnut shells. The produced Ag NPs effectively inhibited both *E. coli* and *S. aureus* bacterial strains. *J. Regia L.* leaf extract serves as a natural antioxidant, effectively mitigating lipid degradation and antioxidant damage to pharmaceuticals, food products, and excipient bases [23]. Additionally, the leaf extract of *J. Regia L.* was employed to synthesize green ZnO NPs for the formulation of a degradable antimicrobial film composed of polyethylene-starch-ZnO NPs [24].

The findings demonstrate that the film formulated with 2% green-sensitized ZnO nanoparticles exhibited significant bactericidal inhibitory effects against *E. coli* and *S. aureus* bacterial strains. In a separate investigation, Sheikhlou et al. [25] utilized *J. Regia L.* walnut leaf extract and microwave irradiation to synthesize selenium nanoparticles (Se NPs) with an average particle size of 150 nm. The results indicate that the green-sensitized Se

nanoparticles show potent bactericidal activity against *E. coli* and *S. aureus*. In contrast, Mohammadi et al. [26] synthesized cobalt oxide ( $\text{Co}_3\text{O}_4$  NPs) with a range of 60–80 nm utilizing walnut green husk extract as a reducer.

According to a review of the literature, a substantial quantity of research is currently published regarding the biosynthesis of copper oxide ( $\text{CuO}$ ) utilizing walnut and its extracts. As an illustration, Barati et al. [27] utilized the aqueous extract from walnut green husks to create  $\text{CuO}$  nanoparticles with a typical diameter of 82.61 nm through green synthesis.

Another study by Abdollahzadeh et al. [28] studied the environmentally friendly production of  $\text{CuO}$  NPs using powdered walnut shell at various calcination temperatures (400–900°C). The cytotoxic effects of the  $\text{CuO}$ -900 NPs on colon and breast cancer cells were encouraging. Lately, Mahmud [5] revealed the  $\text{CuO}@\text{Fe}_3\text{O}_4@\text{walnut shell}$  nanocomposite's biogenesis.

This study reports a new biogenic synthesis of the  $\text{CuO}@\text{CaO}@\text{Fe}_3\text{O}_4$  nanocomposite employing a reducing and stabilizing agent made from *J. Regia L* walnut green extract. The bio-synthesized  $\text{CuO}@\text{CaO}@\text{Fe}_3\text{O}_4$  nanocomposite displayed higher antioxidant activity toward scavenging hydrogen peroxide in comparison with vitamin C. Additionally, the in vitro study confirmed that the prepared  $\text{CuO}@\text{CaO}@\text{Fe}_3\text{O}_4$  nanocomposite exhibited an enhanced capability to address Gram-negative as well as Gram-positive bacteria.

## 2. MATERIALS AND METHODS

### 2.1. Chemicals

The chemicals used in this investigation were of analytical grade quality. Iron (II) chloride tetrahydrate ( $\text{FeCl}_2 \cdot 4\text{H}_2\text{O}$ , 99% purity), ferric chloride hexahydrate ( $\text{FeCl}_3 \cdot 6\text{H}_2\text{O}$ , 97% purity), copper sulfate ( $\text{CuSO}_4$ , 99%), palladium (II) chloride ( $\text{PbCl}_2$ , 59% Pd), hydrogen peroxide ( $\text{H}_2\text{O}_2$ , 34.5–36.5%), ascorbic acid ( $\text{C}_6\text{H}_8\text{O}_6$ ), and were acquired from Sigma-Aldrich.

### 2.2. Nanocomposite Characterization

The *J. Regia L.* extract and the synthesized  $\text{CuO}@\text{CaO}@\text{Fe}_3\text{O}_4$  nanocomposite were characterized using various techniques. UV-Vis measurements were performed with a double beam spectrophotometer (CE9500). Functional groups were identified using FTIR spectroscopy. The FTIR spectrum was obtained via the KBr pellet method with a Nicolet spectrophotometer (Shimadzu) across the 4000–400  $\text{cm}^{-1}$  range, with a resolution of 2  $\text{cm}^{-1}$ . A  $\text{Cu}/\text{K}\alpha$  radiation source ( $\lambda = 0.15406$  nm) was employed, with  $2\theta$  angles ranging from 10° to 70°, using an X-ray diffractometer (X-Pert PRO X-ray) operating at 40 kV and 30 mA to determine the crystal phase of the  $\text{CuO}@\text{CaO}@\text{Fe}_3\text{O}_4$  nanocomposite at a scan rate of 1°/min. Energy dispersive X-ray analysis (EDX) at 20 kV was used for element detection, alongside a field emission scanning electron microscope (FE-SEM: SU8220, Hitachi, Japan) to examine the size and surface morphology of the nanocomposite.

## 3. EXPERIMENTAL PROCEDURES

### 3.1. Plant Materials

*J. Regia L.* green husk was collected from Kore Mountain, Erbil city, Kurdistan, Iraq (GPS coordinates: Latitude 36°24'01.4"N and Longitude 44°14'33.5"E) in September 2023. The optical image of the collected plant with its classifications is presented in Figure 1. The collected plant was dried to a constant weight in shade at  $20^\circ \pm 2^\circ\text{C}$ . The dried sample was ground, and the homogeneous sample was stored for subsequent use.



#### Scientific classification

Kingdome	<i>Plantae</i>
Phylum	<i>Tracheophytes</i>
Class	<i>Angiosperms</i>
Order	<i>Fagales</i>
Family	<i>Juglandaceae</i>
Genus	<i>Juglans</i>
Species	<i>J. Regia L.</i>

**Figure 1.** Optical image depicting the green husk of *J. Regia L.* collected on Kore Mountain, located in Erbil city, Kurdistan, Iraq.

### 3.2. *J. Regia L.* Green Husk Extract and Spectroscopic Analysis

This experiment involved adding 20 g of the dry powder to a round-bottom flask with 100 mL of distilled water, and then refluxing the mixture for 40 minutes at 80°C. Subsequently, the extracted material was filtered, stored in a refrigerator, and analyzed using UV-Vis and FTIR.

### 3.3. Phytochemical Analysis

Samples of the fruit at maturity (September 2023) were utilized to examine the phytochemical makeup of the *J. regia L.* green husk extract. Table 1 displays the major chemicals identified along with their quantities. Precisely, 5 g of dried *J. regia L.* green husk powder was extracted using a 90% ethanolic solution at 70°C with magnetic stirring for 40 minutes. Post-filtration, the obtained filtrate was subjected to phytochemical examination employing standardized methodologies [29].

#### 3.3.1. Phenol and Flavonoid Quantification

Phenol quantification of the extract of *J. regia L.* green husk was estimated according to the Folin-Ciocalteu reagent assay with slight modification [30, 31]. Subsequently, 3.75 ml of distilled water, 0.5 ml of *J. regia L.* extract, and 0.25 ml of Folin-Ciocalteu reagent, diluted 1:1 (v/v) with distilled water, were combined. After one minute of waiting, 0.5 ml of a 10% w/v sodium carbonate solution was added. After a one-hour reaction at room temperature, the absorbance was recorded at 765 nm. Gallic acid was utilized as the reference for the calibration curve (0-100 mg/L). The findings were presented as gallic acid equivalents (GAE) per 100 g of dry weight (DW) of walnut green husk. With certain adjustments, the total flavonoid content (TFC) was calculated using [32]. To summarize, 1.5 mL of methanol was mixed with 0.1 mL of plant extract (0.1 g/mL) and agitated for 5 minutes. Subsequently, 2.8 mL of distilled water (DW), 0.1 mL of CH<sub>3</sub>COOK (1 M), and 0.1 mL of AlCl<sub>3</sub> (10%) were incorporated into the mixture. Using a quercetin reference, TFC was spectrophotometrically quantified at 410 nm as QE/g dry plant after 30 minutes.

#### 3.3.2. Hydrogen Peroxide Scavenging Activity

Based on earlier research, the hydrogen peroxide scavenging activity was examined [33, 34]. In brief, 1 mL of hydrogen peroxide solution (40 mM, pH 7.4) was combined with 0.6 mL of extract (0.1 g/mL). The synthesized CuO@CaO@Fe<sub>3</sub>O<sub>4</sub> nanocomposite was subsequently introduced into a hydrogen peroxide solution at different concentrations ranging from 1000 to 200 µg/mL. Following a ten-minute interval, the absorbance of the solution at 230 nm was measured against a blank solution containing phosphate buffer devoid of H<sub>2</sub>O<sub>2</sub>. Equation 1 was used to assess the H<sub>2</sub>O<sub>2</sub> scavenging activity [28].

$$H_2O_2 \text{ scavenging activity (\%)} = \frac{A_0 - A}{A_0} \times 100 \quad (1)$$

In this context,  $A_0$  represents the absorbance of the control sample, while  $A$  denotes the absorbance observed in the presence of the samples.

### 3.4. Green Synthesis of the $CuO@CaO@Fe_3O_4$ Nanocomposite

The  $CuO@CaO@Fe_3O_4$  nanocomposite was prepared through a green synthesis route using *J. Regia L.* green husk extract. In the initial phase, 20 g of dried plant material was combined with 200 mL of double distilled water (DW) and maintained at 80 °C for 40 minutes to extract the green husk. The extract was then mixed with aqueous solutions of  $FeCl_2$  and  $FeCl_3$  in a molar ratio of 1:2. The pH of the solution was adjusted to 11. Subsequently, the mixture was heated at 50 °C for 60 minutes using a magnetic stirrer. Following this, the mixture was refluxed for two hours at 70 °C with the addition of 1 g of  $Ca(NO_3)_2$  and 0.75 g of  $Cu(NO_3)_2$ . The resulting  $CuO@CaO@Fe_3O_4$  nanocomposite was separated using an external magnet, then washed at least three times with ethanol (EtOH) and hot double-distilled water. The washed sample was dried in an oven at 60°C for 12 hours. Finally, the  $CuO@CaO@Fe_3O_4$  nanocomposite was stored in sample tubes for characterization and further investigations.

### 3.5. Antimicrobial Activity

Utilizing the agar well diffusion method, the antimicrobial properties of green husk extract of *J. regia L.* and the produced  $CuO@CaO@Fe_3O_4$  nanocomposite were examined [35]. The microbial species, including both Gram-negative and Gram-positive lag phase cultures, were employed as test microorganisms, in contrast to common bacterial isolates such as *Escherichia coli* (*E. coli*), *Pseudomonas aeruginosa* (*P. aeruginosa*), *Salmonella typhimurium* (*S. typhimurium*), and *Staphylococcus aureus* (*S. aureus*). The discs were incubated for two hours at 37 °C after being submerged in plant extract at concentrations of 100%, 50%, and 12.5%, and in  $CuO@CaO@Fe_3O_4$  nanocomposite at concentrations of 100 mg/ml, 50 mg/ml, and 10 mg/ml. Following a 24-hour incubation at 37 °C, the plates were immediately covered with disks infused with samples and distilled water (negative control). The antibacterial activity of the produced nanoparticles was then observed and measured. The zones of inhibition were quantified in millimeters using a standard scale [4].

## 4. RESULTS AND DISCUSSION

### 4.1. Phytochemical Screening of *J. Regia L.* Green Husk Extract

Qualitative phytochemical analysis of *J. regia L.* extraction disclosed the existence of carbohydrates, alkaloids, phenolic compounds, flavonoids, tannins, diterpenes, triterpenoids, steroids, glycosides, coumarins, and saponins, as shown in Table 1.

**Table 1.** Phytochemical screening of *J. regia L.* green husk extract.

Active constituents	Chemical tests	Results	Observation
Carbohydrates	Molisch's test	+++	Violet ring
	Benedict's test	+++	Red ppt
Protein and amino acids	Ninhydrin test	+	Violet ppt
	Dragendorff's test	++	Red ppt
Alkaloids	Wagner's test	+	Brown ppt
	Ferric chloride test	+	Green color
Phenolic compounds	Lead acetate test	++++	Yellow color
Flavonoids	Gelatin test	-	White ppt
Tannins	Liberman-Burchard test	++	Green color
Detection of steroids and triterpenoids	Aqueous mercury chloride	+	White ppt
Saponins	Keller-Kilian's test	++	Green Color

#### 4.2. Phenol and Flavonoid Quantification of *J. regia L.* Green Husk

The TPC and TFC of *J. regia L.* green husk were spectrophotometrically estimated. The findings in Table 2 demonstrate the existence of phenolics, such as taxifolin, salicylate glucuronide, quercetin isomers, and catechin, and indicate that the plant extract is a potent source of polyphenolics. Alternatively, Nour et al. [36] reported that using high-performance liquid chromatography, the walnut leaves are free of juglone, flavonoids (rutin, epicatechin, catechin, quercetin, and myricetin), and phenolic acids (vanillic, chlorogenic, gallic, caffeic, syringic, p-coumaric, sinapic, salicylic, ferulic, and trans-cinnamic acid, ellagic) [36].

**Table 2.** Total phenol and flavonoid content of *J. regia L.* green husk extract.

Taster	TPC (µg GAE/500 µg extract)	TFC (µg QE/500 µg extract)
J. Regia L. Green Husk extract	62.67 ± 0.01	38.61 ± 0.01

#### 4.3. UV-Visible Spectroscopy

The UV-Visible spectroscopy of the *J. Regia L.* extract showed two broad bands at 264.2 nm and 335.6 nm, as shown in Figure 2. The band at lower wavelength is attributed to bonds, and the band at higher wavelength is assigned to bond I for the benzoyl and cinnamoyl phenolic systems. These are associated with the  $\pi \rightarrow \pi^*$  electronic transition, demonstrating that polyphenols are present as antioxidant free radicals throughout the environmentally friendly synthesis of nanoparticles. The CuO@CaO@Fe<sub>3</sub>O<sub>4</sub> nanocomposite, which was created using plant extract, showed a small band at 230 nm in its UV-Visible spectra.

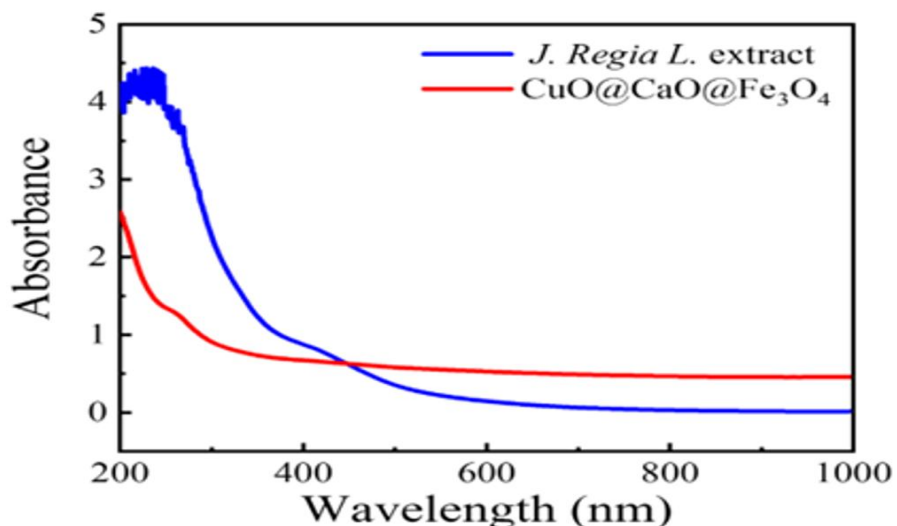


**Figure 2.** UV-Vis spectra of the CuO@CaO@Fe<sub>3</sub>O<sub>4</sub> nanocomposite and green husk extract from *J. Regia L.*

#### 4.4. FTIR Spectroscopy

Figure 3 presents the FTIR spectra of the CuO@CaO@Fe<sub>3</sub>O<sub>4</sub> nanocomposite and *J. Regia L.* green husk, scanned over wavenumbers ranging from 4000 to 400 cm<sup>-1</sup>. Strong peaks associated with the C-H stretching of CH<sub>2</sub> and OH groups, respectively, were observed in the spectra of *J. Regia L.* green husk and the CuO@CaO@Fe<sub>3</sub>O<sub>4</sub> nanocomposite at 3050–2801 cm<sup>-1</sup> and 3600–3300 cm<sup>-1</sup>. This indicates the presence of phenolic compounds. The occurrence of phenolic compounds is further confirmed by the aromatic C=O groups, which are indicated by the small broad signal at 1598 cm<sup>-1</sup>. The C=O and C-O groups contribute to the small vibrational bands at 1116 and 1239 cm<sup>-1</sup>, respectively. The octahedral Fe-O and the inherent vibration of the tetrahedral Fe-O bonds are recognized by the tiny bands at 4018 and 603 cm<sup>-1</sup>, respectively [37]. The minor peaks at 525 and 584 cm<sup>-1</sup> correspond to the Cu-O stretching modes [38, 39]. The CO groups are indicated by bands at 1417 and 866 cm<sup>-1</sup>, while the CaO groups are

indicated by bands at approximately 553 and 427 cm<sup>-1</sup> [40]. These bands' existence attests to the CuO@CaO@Fe<sub>3</sub>O<sub>4</sub> nanocomposite's good preparation.

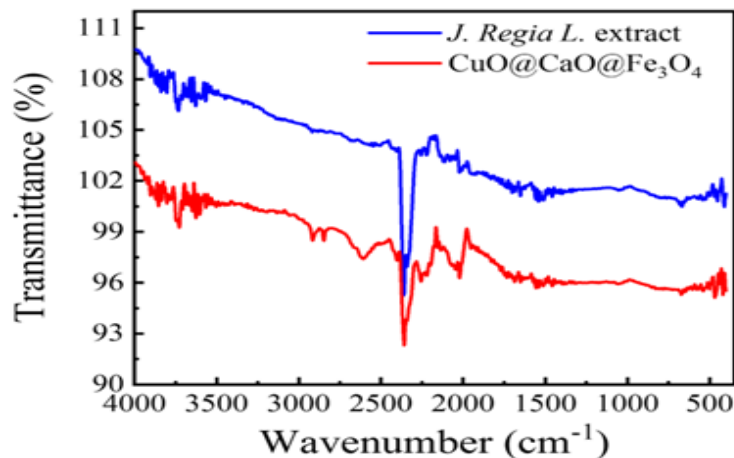


Figure 3. FTIR spectrum of *J. Regia L.* green husk and CuO@CaO@Fe<sub>3</sub>O<sub>4</sub> nanocomposite.

#### 4.5. Characterization of CuO@CaO@Fe<sub>3</sub>O<sub>4</sub> Nanocomposite

SEM has been used to depict the morphologies of the green-generated CuO@CaO@Fe<sub>3</sub>O<sub>4</sub> nanocomposite to observe the samples' surfaces. The presence of particle clusters and the predominance of spherical particles were visible in the low-magnification SEM microstructure images (Figure 4a, 4b). The high-magnification SEM microstructure image of the CuO@CaO@Fe<sub>3</sub>O<sub>4</sub> nanocomposite is displayed in Figure 4c. It is observed that the synthesized CuO@CaO@Fe<sub>3</sub>O<sub>4</sub> nanocomposite exhibits a sphere-like structure. As shown in Figure 4d, the estimated particle sizes from SEM images range from 80 to 120 nm, with an average size of 90 nm.

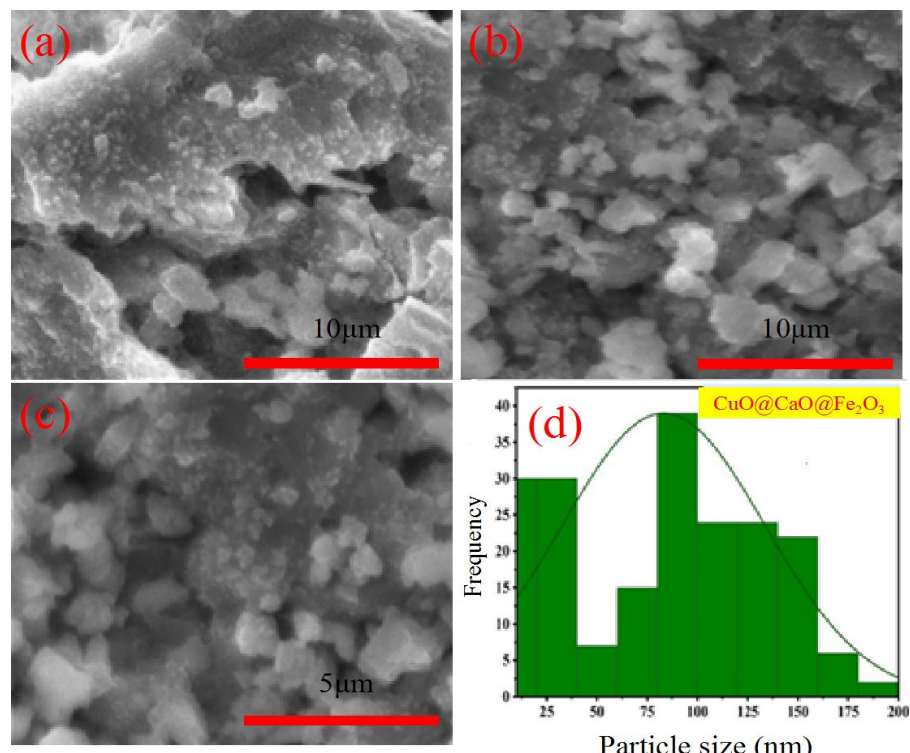


Figure 4. SEM images of CuO@CaO@Fe<sub>3</sub>O<sub>4</sub> nanocomposite. (a-b) Low magnification SEM images and (c) high magnification SEM images of the green synthesized CuO@CaO@Fe<sub>3</sub>O<sub>4</sub> nanocomposite. (d) Histogram for particle size distribution from SEM images.

The phase purity and elemental composition of the CuO@CaO@Fe<sub>3</sub>O<sub>4</sub> nanocomposite were demonstrated through EDX analysis. The elements Cu, Ca, Fe, and O were identified in the EDX spectrum shown in Figure 5a. Regarding chemical constituents, the atomic percentages of the sensitized CuO@CaO@Fe<sub>3</sub>O<sub>4</sub> nanocomposite are 27.99% Ca, 1.46% Cu, 16.03% Fe, and 48.55% O. Furthermore, as illustrated in Figure 5b, the elemental mapping confirms the uniform distribution of Cu, Ca, Fe, and O elements. These findings collectively validate the successful synthesis of the green CuO@CaO@Fe<sub>3</sub>O<sub>4</sub> nanocomposite, demonstrating its phase purity and elemental homogeneity, which are critical for its potential applications in various fields such as catalysis, environmental remediation, and magnetic materials.

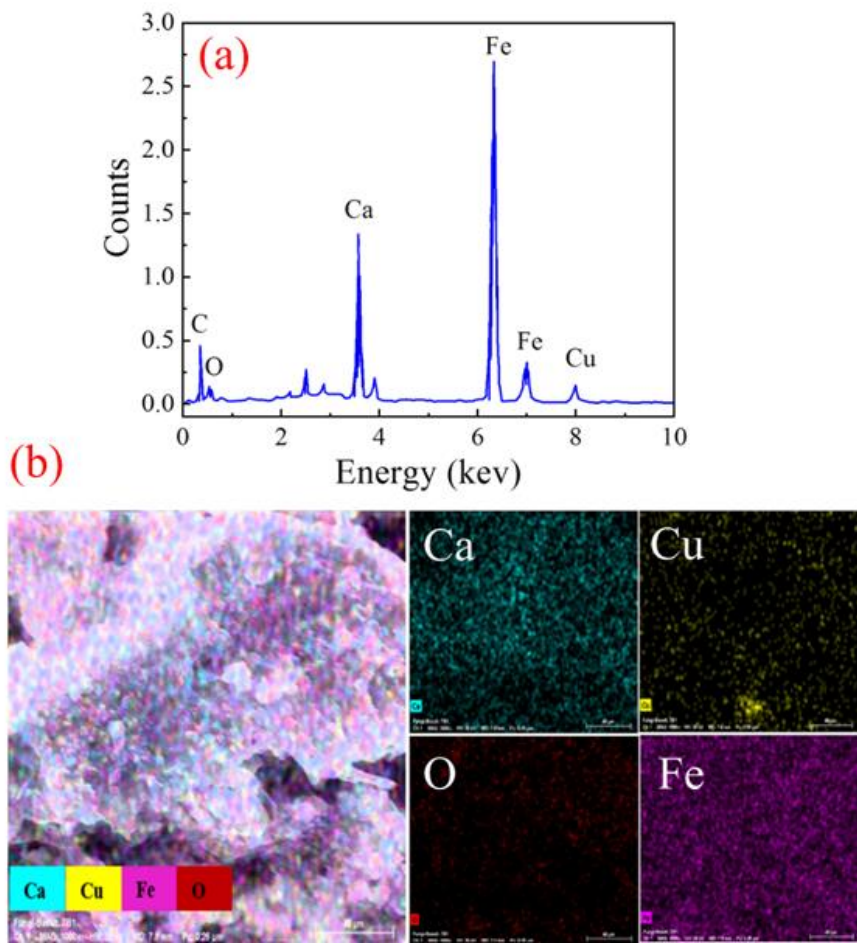
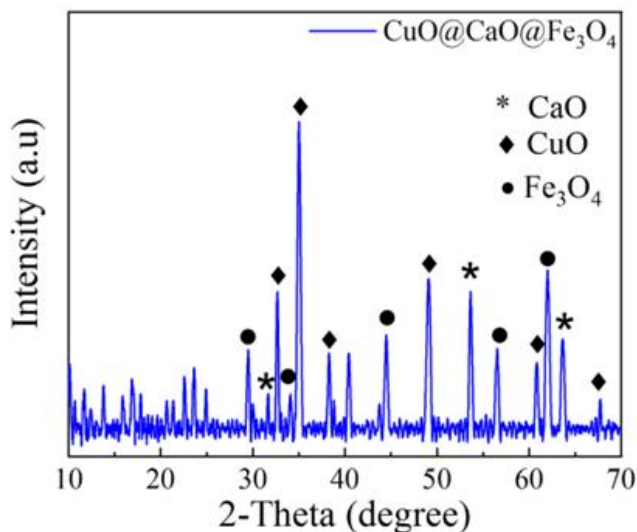


Figure 5. (a) EDX-line and (b) EDX mapping for the synthesized CuO@CaO@Fe<sub>3</sub>O<sub>4</sub> nanocomposite.

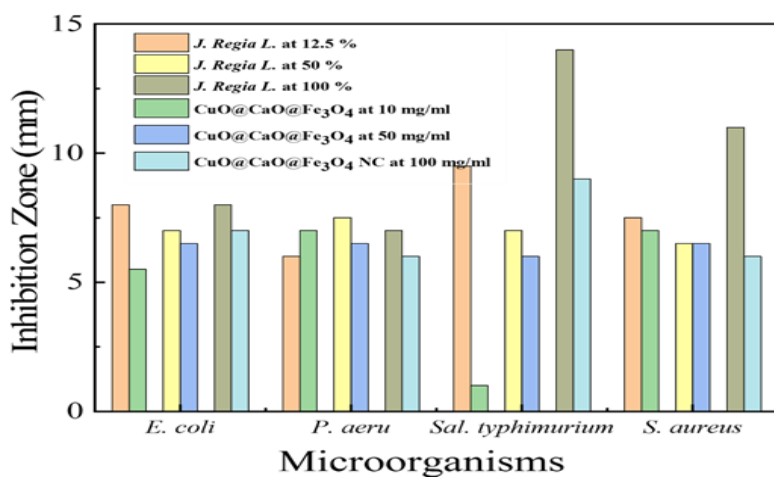
XRD was used to examine the phase elements of the CuO@CaO@Fe<sub>3</sub>O<sub>4</sub> nanocomposite, as illustrated in Figure 6. According to JCPDS PDF # 74-1226, the (111), (200), and (311) planes of CaO were ascribed to the diffraction peaks that emerged at 32.4°, 54.3°, and 64.6° [41], while the peaks of diffraction occurring at  $2\theta = 32.6^\circ, 35.6^\circ, 38.8^\circ, 48.8^\circ, 61.6^\circ, 66.3^\circ$ , and  $68.2^\circ$  were assigned to the planes (110), (-111), (111), (-202), (-113), (-311), and (220), respectively. These are highly consistent with CuO with a monoclinic phase (JCPDS PDF# 01-080-0076) [42]. The crystal faces of Fe<sub>3</sub>O<sub>4</sub> (220), (311), (400), (422), (511), and (440) are represented by peaks at  $2\theta$  of 30.3°, 35.4°, 43.4°, 53.5°, 56.9°, and 62.6°, respectively, aligning with the JCPDS PDF 03-0863 standard PDF card [43]. The presence of the CaO, CuO, and Fe<sub>3</sub>O<sub>4</sub> planes confirms the successful synthesis of the CuO@CaO@Fe<sub>3</sub>O<sub>4</sub> nanocomposite. The average crystallite size of the nanocomposite, which is on a nanoscale, is 16 nm, as determined by applying the Debye-Scherrer equation [44].

Figure 6. XRD pattern of the green sensitized CuO@CaO@Fe<sub>3</sub>O<sub>4</sub> nanocomposite.

#### 4.6. Antimicrobial Activity

Both types of bacteria, including *B. subtilis*, *S. aureus*, *E. coli*, and *P. aeruginosa*, were evaluated using the disk diffusion method to assess the antibacterial efficacy of the CuO@CaO@Fe<sub>3</sub>O<sub>4</sub> nanocomposite and *J. regia L* extract. The results demonstrated high antibacterial activity. Figure 7 illustrates the bacterial zone of inhibition caused by the impact of *J. regia L* extract and the CuO@CaO@Fe<sub>3</sub>O<sub>4</sub> nanocomposite at different concentrations. Both *J. regia L* extract and the CuO@CaO@Fe<sub>3</sub>O<sub>4</sub> nanocomposite exhibited antimicrobial effectiveness against a variety of bacteria, including both Gram-negative and Gram-positive strains, according to the results. It has been shown that the size of the zone of inhibition for *E. coli* increased with increasing concentrations of the CuO@CaO@Fe<sub>3</sub>O<sub>4</sub> nanocomposite. Conversely, no significant increase was observed with *J. regia L* extract, and a decrease of 50% was noted. Additionally, both *J. regia L* and the synthesized CuO@CaO@Fe<sub>3</sub>O<sub>4</sub> nanocomposite displayed a notable expansion of the zone of inhibition for *S. typhimurium*. The antimicrobial activity of the CuO@CaO@Fe<sub>3</sub>O<sub>4</sub> nanocomposite against *S. aureus* decreased with increasing concentration, as indicated by the reduction in the size of the inhibitory zone.

To conclude these findings, the prepared CuO@CaO@Fe<sub>3</sub>O<sub>4</sub> nanocomposite exhibited higher antimicrobial activity against *S. typhimurium* and *E. coli* bacteria. According to the FTIR spectra (Figure 3), a higher concentration of bioactive phytochemicals adsorbed on the CuO@CaO@Fe<sub>3</sub>O<sub>4</sub> nanocomposite's vast surface area is most likely responsible for this result.

Figure 7. Antibacterial inhibition zone (mm) of the CuO@CaO@Fe<sub>3</sub>O<sub>4</sub> nanocomposite inhibition of both types of bacteria at varying concentrations.

#### 4.7. Scavenging Activity

In this case, the scavenging capacity of hydroxyl radicals was assessed through an examination of the antioxidant activity using  $H_2O_2$ . As seen in Figure 8, the scavenging activity increased as the  $CuO@CaO@Fe_3O_4$  nanocomposite concentration increased, which is consistent with findings reported by Veeramanikandan et al. [45]. Traditional phytochemical analysis and polyphenolic compound quantification of the plant indicated the potent antioxidant activity of *J. regia* L. green husk extract to scavenge  $H_2O_2$  compared to vitamin C. The presence of phenolic compounds in the samples is the primary determinant of the  $H_2O_2$  test [3]. One class of antioxidant agents known to be effective at donating protons is phenolic chemicals, which also function as free radical terminators and enhance the antioxidant properties of plants. The potential scavenging activity of the produced  $CuO@CaO@Fe_3O_4$  nanocomposite to scavenge  $H_2O_2$  is due to the antioxidant phytoconstituents from the plant that are deposited on its surface.

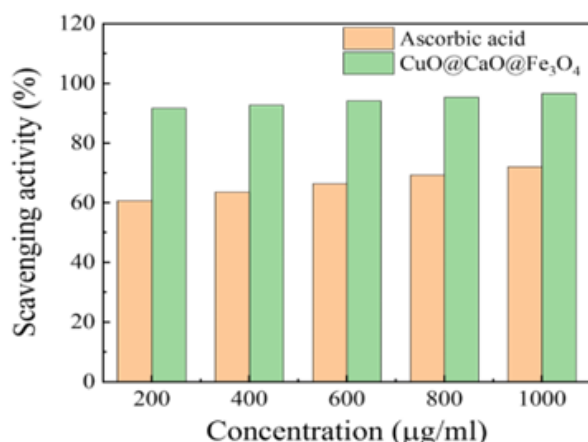


Figure 8.  $H_2O_2$  degrading properties of  $CuO@CaO@Fe_3O_4$  nanocomposite at various concentrations.

## 5. CONCLUSION

The aqueous extract of *J. regia* L. walnut green husk has been successfully used as a biological mediator for the biosynthesis of a cubic-orthorhombic  $CuO@CaO@Fe_3O_4$  nanocomposite, featuring a mean particle diameter of 90 nm. The walnut husk extract and the prepared nanocomposites demonstrate antimicrobial efficacy, with robust assessments against prominent pathogens including *Staphylococcus aureus*, *Pseudomonas aeruginosa*, and *Escherichia coli*. The nanocomposites exhibit significant antioxidant properties through the  $H_2O_2$  process. These findings highlight their potential to mitigate oxidative stress and cellular damage, positioning them as promising candidates in preventive healthcare and longevity promotion. Future work will focus on assessing the cytotoxicity of the synthesized  $CuO@CaO@Fe_3O_4$  nanocomposite in appropriate cell lines, along with conducting in vivo studies to further evaluate its biological applications and safety profile. This study aims to deepen the understanding of the therapeutic and industrial applications of this eco-friendly nanocomposite.

**Funding:** This study received no specific financial support.

**Institutional Review Board Statement:** Not applicable.

**Transparency:** The authors state that the manuscript is honest, truthful, and transparent, that no key aspects of the investigation have been omitted, and that any differences from the study as planned have been clarified. This study followed all writing ethics.

**Competing Interests:** The authors declare that they have no competing interests.

**Authors' Contributions:** All authors contributed equally to the conception and design of the study. All authors have read and agreed to the published version of the manuscript.

**Disclosure of AI Use:** The authors used OpenAI's ChatGPT (GPT-5 mini) only in limited instances to assist with minor grammatical corrections. All outputs generated by the AI were carefully reviewed, verified, and edited by the authors to ensure scientific accuracy and clarity.

## REFERENCES

[1] P. Dwivedi *et al.*, "Eco-friendly CuO/Fe<sub>3</sub>O<sub>4</sub> nanocomposite synthesis, characterization, and cytotoxicity study," *Helijon*, vol. 10, no. 6, p. e27787, 2024. <https://doi.org/10.1016/j.helijon.2024.e27787>

[2] B. Ates, S. Koytepe, A. Ulu, C. Gurses, and V. K. Thakur, "Chemistry, structures, and advanced applications of nanocomposites from biorenewable resources," *Chemical Reviews*, vol. 120, no. 17, pp. 9304-9362, 2020. <https://doi.org/10.1021/acs.chemrev.9b00553>

[3] D. Bharathi, R. Ranjithkumar, S. Vasantharaj, B. Chandarshekhar, and V. Bhuvaneshwari, "Synthesis and characterization of chitosan/iron oxide nanocomposite for biomedical applications," *International Journal of Biological Macromolecules*, vol. 132, pp. 880-887, 2019. <https://doi.org/10.1016/j.ijbiomac.2019.03.233>

[4] R. Golabiazzar, A. R. Alee, S. F. Mala, Z. A. Omar, H. S. Abdulmanaf, and K. M. Khalid, "Investigating kinetic, thermodynamic, isotherm, antibacterial activity and paracetamol removal from aqueous solution using AgFe<sub>3</sub>O<sub>4</sub> nanocomposites synthesized with sumac plant extract," *Journal of Cluster Science*, vol. 34, no. 5, pp. 2547-2564, 2023. <https://doi.org/10.1007/s10876-023-02406-x>

[5] S. A. Mahmud, "Green synthesis of bioactive CuO@Fe<sub>3</sub>O<sub>4</sub>@Walnut shell nanocomposite using Crataegus azarolus var. Aronia L. Extract and its antivasoconstrictive action on rat's aortic smooth muscle," *Polytechnic Journal*, vol. 11, no. 1, pp. 118-125, 2021. <https://doi.org/10.25156/ptj.v11n1y2021.pp118-125>

[6] K. J. Anderson, S. S. Teuber, A. Gobeille, P. Cremin, A. L. Waterhouse, and F. M. Steinberg, "Walnut polyphenolics inhibit in vitro human plasma and LDL oxidation," *The Journal of Nutrition*, vol. 131, no. 11, pp. 2837-2842, 2001. <https://doi.org/10.1093/jn/131.11.2837>

[7] B. K. Aithal, M. S. R. Kumar, B. N. Rao, N. Udupa, and B. S. Rao, "Juglone, a naphthoquinone from walnut, exerts cytotoxic and genotoxic effects against cultured melanoma tumor cells," *Cell Biology International*, vol. 33, no. 10, pp. 1039-1049, 2009. <https://doi.org/10.1016/j.cellbi.2009.06.018>

[8] M. T. Paulsen and M. Ljungman, "The natural toxin juglone causes degradation of p53 and induces rapid H2AX phosphorylation and cell death in human fibroblasts," *Toxicology and Applied Pharmacology*, vol. 209, no. 1, pp. 1-9, 2005. <https://doi.org/10.1016/j.taap.2005.03.005>

[9] S. Barathi, R. D. S. Vardhini, P. Chitra, and P. I. Arulselvi, "Cytotoxic effect of juglone on human peripheral blood lymphocytes," *Asian Journal of Pharmaceutical and Clinical Research*, vol. 6, no. 4, pp. 178-186, 2013.

[10] V. V. Makarov *et al.*, "Green nanotechnologies: Synthesis of metal nanoparticles using plants," *Acta Naturae*, vol. 6, no. 1 (20), pp. 35-44, 2014. <https://doi.org/10.32607/20758251-2014-6-1-35-44>

[11] S. Ying *et al.*, "Green synthesis of nanoparticles: Current developments and limitations," *Environmental Technology & Innovation*, vol. 26, p. 102336, 2022. <https://doi.org/10.1016/j.eti.2022.102336>

[12] N. Ramezani, F. Raji, M. Rezakazemi, and M. Younas, "Juglone extraction from walnut (*Juglans regia L.*) green husk by supercritical CO<sub>2</sub>: Process optimization using Taguchi method," *Journal of Environmental Chemical Engineering*, vol. 8, no. 3, p. 103776, 2020. <https://doi.org/10.1016/j.jece.2020.103776>

[13] G. Park, D. S. Jang, and M. S. Oh, "Juglans mandshurica leaf extract protects skin fibroblasts from damage by regulating the oxidative defense system," *Biochemical and Biophysical Research Communications*, vol. 421, no. 2, pp. 343-348, 2012. <https://doi.org/10.1016/j.bbrc.2012.04.013>

[14] J. R. Vergara-Salinas, M. Vergara, C. Altamirano, Á. Gonzalez, and J. R. Pérez-Correa, "Characterization of pressurized hot water extracts of grape pomace: Chemical and biological antioxidant activity," *Food Chemistry*, vol. 171, pp. 62-69, 2015. <https://doi.org/10.1016/j.foodchem.2014.08.094>

[15] E. Conde, C. Cara, A. Moure, E. Ruiz, E. Castro, and H. Domínguez, "Antioxidant activity of the phenolic compounds released by hydrothermal treatments of olive tree pruning," *Food Chemistry*, vol. 114, no. 3, pp. 806-812, 2009. <https://doi.org/10.1016/j.foodchem.2008.10.017>

[16] M. Zabihi, A. Ahmadpour, and A. H. Asl, "Removal of mercury from water by carbonaceous sorbents derived from walnut shell," *Journal of Hazardous Materials*, vol. 167, no. 1-3, pp. 230-236, 2009. <https://doi.org/10.1016/j.jhazmat.2008.12.108>

[17] C. Soto-Maldonado *et al.*, "Polyphenolic extracts of walnut (*Juglans regia*) green husk containing juglone inhibit the growth of HL-60 cells and induce apoptosis," *Electronic Journal of Biotechnology*, vol. 39, pp. 1-7, 2019. <https://doi.org/10.1016/j.ejbt.2019.02.001>

[18] N. A. Taha and M. A. Al-wadaan, "Utility and importance of walnut, *Juglans regia* Linn: A review," *African Journal of Microbiological Research*, vol. 5, no. 32, pp. 5796-5805, 2011.

[19] N. Panth, K. R. Paudel, and R. Karki, "Phytochemical profile and biological activity of *Juglans regia*," *Journal of Integrative Medicine*, vol. 14, no. 5, pp. 359-373, 2016. [https://doi.org/10.1016/S2095-4964\(16\)60274-1](https://doi.org/10.1016/S2095-4964(16)60274-1)

[20] E. H. Elshazly *et al.*, "Phytotoxicity and antimicrobial activity of green synthesized silver nanoparticles using nigella sativa seeds on wheat seedlings," *Journal of Chemistry*, vol. 2022, no. 1, p. 9609559, 2022. <https://doi.org/10.1155/2022/9609559>

[21] A. Bouafia, S. E. Laouini, M. L. Tedjani, G. A. M. Ali, and A. Barhoum, "Green biosynthesis and physicochemical characterization of  $\text{Fe}_3\text{O}_4$  nanoparticles using *Punica granatum* L. fruit peel extract for optoelectronic applications," *Textile Research Journal*, vol. 92, no. 15-16, pp. 2685-2696, 2021. <https://doi.org/10.1177/00405175211006671>

[22] İ. Erdem and Ş. Çakır, "Green synthesis of silver nanoparticles using walnut shell powder and cynara sp. and their antibacterial activities," *Hacettepe Journal of Biology and Chemistry*, vol. 50, no. 4, pp. 335-347, 2022. <https://doi.org/10.15671/hjbc.984727>

[23] I. F. Almeida, E. Fernandes, J. L. F. C. Lima, P. C. Costa, and M. F. Bahia, "Walnut (*Juglans regia*) leaf extracts are strong scavengers of pro-oxidant reactive species," *Food Chemistry*, vol. 106, no. 3, pp. 1014-1020, 2008. <https://doi.org/10.1016/j.foodchem.2007.07.017>

[24] R. Saemi, E. Taghavi, H. Jafarizadeh-Malmiri, and N. Anarjan, "Fabrication of green  $\text{ZnO}$  nanoparticles using walnut leaf extract to develop an antibacterial film based on polyethylene-starch- $\text{ZnO}$  NPs," *Green Processing and Synthesis*, vol. 10, no. 1, pp. 112-124, 2021. <https://doi.org/10.1515/gps-2021-0011>

[25] K. Sheikhlou, S. Allahyari, S. Sabouri, Y. Najian, and H. Jafarizadeh-Malmiri, "Walnut leaf extract-based green synthesis of selenium nanoparticles via microwave irradiation and their characteristics assessment," *Open Agriculture*, vol. 5, no. 1, pp. 227-235, 2020. <https://doi.org/10.1515/opag-2020-0024>

[26] S. Z. Mohammadi, B. Lashkari, and A. Khosravan, "Green synthesis of  $\text{Co}_3\text{O}_4$  nanoparticles by using walnut green skin extract as a reducing agent by using response surface methodology," *Surfaces and Interfaces*, vol. 23, p. 100970, 2021. <https://doi.org/10.1016/j.surfin.2021.100970>

[27] F. Barati, F. Hosseini, P. Ghadam, and S. S. Arab, "Optimizing  $\text{CuO}$  nanoparticle synthesis via walnut green husk extract utilizing response surface methodology," *Journal of Molecular Structure*, vol. 1316, p. 139077, 2024. <https://doi.org/10.1016/j.molstruc.2024.139077>

[28] H. Abdollahzadeh, Y. Pazhang, A. Zamani, and Y. Sharafi, "Green synthesis of copper oxide nanoparticles using walnut shell and their size dependent anticancer effects on breast and colorectal cancer cell lines," *Scientific Reports*, vol. 14, no. 1, p. 20323, 2024. <https://doi.org/10.1038/s41598-024-71234-4>

[29] M. K. Kumar, G. Kaur, and H. Kaur, "Synthesis and characterization of pharmaceutical compounds," *Internationale Pharmaceutica Sciencia*, vol. 5, no. 2, pp. 123-130, 2011.

[30] M. R. Rover and R. C. Brown, "Quantification of total phenols in bio-oil using the Folin-Ciocalteu method," *Journal of Analytical and Applied Pyrolysis*, vol. 104, pp. 366-371, 2013. <https://doi.org/10.1016/j.jaap.2013.06.011>

[31] C. Soto, E. Caballero, E. Pérez, and M. E. Zúñiga, "Effect of extraction conditions on total phenolic content and antioxidant capacity of pretreated wild *Peumus boldus* leaves from Chile," *Food and Bioproducts Processing*, vol. 92, no. 3, pp. 328-333, 2014. <https://doi.org/10.1016/j.fbp.2013.06.002>

[32] K. A. Lombard, E. Geoffriau, and E. Peffley, "Flavonoid quantification in onion by spectrophotometric and high performance liquid chromatography analysis," *HortScience*, vol. 37, no. 4, pp. 682-685, 2002. <https://doi.org/10.21273/HORTSCI.37.4.682>

[33] A. K. Keshari, A. Srivastava, S. Chowdhury, and R. Srivastava, "Green synthesis of silver nanoparticles using catharanthus roseus: Its antioxidant and antibacterial properties," *Nanomedicine Research Journal*, vol. 6, no. 1, pp. 17-27, 2021. <https://doi.org/10.22034/nmrj.2021.01.003>

[34] A. A. Al-Amiry, Y. K. Al-Majedy, A. A. H. Kadhum, and A. B. Mohamad, "Hydrogen peroxide scavenging activity of novel coumarins synthesized Using different approaches," *PLoS One*, vol. 10, no. 7, p. e0132175, 2015. <https://doi.org/10.1371/journal.pone.0132175>

[35] M. S. Jadhav, S. Kulkarni, P. Raikar, D. A. Barretto, S. K. Vootla, and U. S. Raikar, "Green biosynthesis of CuO & Ag-CuO nanoparticles from Malus domestica leaf extract and evaluation of antibacterial, antioxidant and DNA cleavage activities," *New Journal of Chemistry*, vol. 42, no. 1, pp. 204-213, 2018. <https://doi.org/10.1039/C7NJ02977B>

[36] V. Nour, I. Trandafir, and S. Cosmulescu, "HPLC determination of phenolic acids, flavonoids and Juglone in walnut leaves," *Journal of Chromatographic Science*, vol. 51, no. 9, pp. 883-890, 2013. <https://doi.org/10.1093/chromsci/bms180>

[37] S. Husain, M. Irfansyah, N. H. Haryanti, S. Suryajaya, S. Arjo, and A. Maddu, "Synthesis and characterization of Fe<sub>3</sub>O<sub>4</sub> magnetic nanoparticles from iron ore," *Journal of Physics: Conference Series*, vol. 1242, no. 1, p. 012021, 2019. <https://doi.org/10.1088/1742-6596/1242/1/012021>

[38] K. Phiwdang, S. Suphankij, W. Mekprasart, and W. Pecharapa, "Synthesis of CuO nanoparticles by precipitation method using different precursors," *Energy Procedia*, vol. 34, pp. 740-745, 2013. <https://doi.org/10.1016/j.egypro.2013.06.808>

[39] R. Bai *et al.*, "Rapid and efficient removal of naproxen from water by CuFe<sub>2</sub>O<sub>4</sub> with peroxymonosulfate," *Environmental Science and Pollution Research*, vol. 27, no. 17, pp. 21542-21551, 2020. <https://doi.org/10.1007/s11356-020-08613-7>

[40] A. Roy and J. Bhattacharya, "Microwave-assisted synthesis and characterization of CaO nanoparticles," *International Journal of Nanoscience*, vol. 10, no. 03, pp. 413-418, 2011. <https://doi.org/10.1142/S0219581X11008150>

[41] J. Liu *et al.*, "Conversion of Au(III)-polluted waste eggshell into functional CaO/Au nanocatalyst for biodiesel production," *Green Energy & Environment*, vol. 7, no. 2, pp. 352-359, 2022. <https://doi.org/10.1016/j.gee.2020.07.019>

[42] H. Veisi, B. Karmakar, T. Tamoradi, S. Hemmati, M. Hekmati, and M. Hamelian, "Biosynthesis of CuO nanoparticles using aqueous extract of herbal tea (*Stachys Lavandulifolia*) flowers and evaluation of its catalytic activity," *Scientific Reports*, vol. 11, no. 1, p. 1983, 2021. <https://doi.org/10.1038/s41598-021-81320-6>

[43] J. Xu, Y. Sun, and J. Zhang, "Solvothermal synthesis of Fe<sub>3</sub>O<sub>4</sub> nanospheres for high-performance electrochemical non-enzymatic glucose sensor," *Scientific Reports*, vol. 10, no. 1, p. 16026, 2020. <https://doi.org/10.1038/s41598-020-73090-4>

[44] A. L. Patterson, "The scherrer formula for X-ray particle size determination," *Physical Review*, vol. 56, no. 10, pp. 978-982, 1939.

[45] V. Veeramanikandan, G. Madhu, V. Pavithra, K. Jaianand, and P. Balaji, "Green synthesis, characterization of iron oxide nanoparticles using *Leucas aspera* leaf extract and evaluation of antibacterial and antioxidant studies," *International Journal of Agriculture Innovations and Research*, vol. 6, no. 02, pp. 242-250, 2017.

*Views and opinions expressed in this article are the views and opinions of the author(s), Journal of Asian Scientific Research shall not be responsible or answerable for any loss, damage or liability etc. caused in relation to/arising out of the use of the content.*